

**A major purpose of the Technical Information Center is to provide the broadest dissemination possible of information contained in DOE's Research and Development Reports to business, industry, the academic community, and federal, state and local governments.**

**Although a small portion of this report is not reproducible, it is being made available to expedite the availability of information on the research discussed herein.**

**1**

PORTIONS OF THIS REPORT ARE ILLICIBLE. It has been reproduced from the best available copy to permit the broadest possible availability.

Los Alamos National Laboratory is operated by the University of California for the United States Department of Energy under contract W-7405-ENG-38

TITLE: DESIGN AND OPERATING EXPERIENCE OF AN AC-DC POWER CONVERTER FOR A SUPERCONDUCTING MAGNETIC ENERGY STORAGE UNIT

AUTHOR(S): H. J. Boenig, CTR-4  
R. G. Nielsen, Bonneville Power Administration  
K. H. Sueker, Robicon Corporation

LA-UR--84-1949

DE84 014041

SUBMITTED TO IEEE Industry Applications Society 1984 Meeting  
Chicago, Illinois  
October 1-4, 1984

MASTER

DISCLAIMER

This report was prepared as an account of work sponsored by an agency of the United States Government. Neither the United States Government nor any agency thereof, nor any of their employees, makes any warranty, express or implied, or assumes any legal liability or responsibility for the accuracy, completeness, or usefulness of any information, apparatus, product, or process disclosed, or represents that its use would not infringe privately owned rights. Reference herein to any specific commercial product, process, or service by trade name, trademark, manufacturer, or otherwise does not necessarily constitute or imply its endorsement, recommendation, or favoring by the United States Government or any agency thereof. The views and opinions of authors expressed herein do not necessarily state or reflect those of the United States Government or any agency thereof.

By acceptance of this article, the publisher recognizes that the U.S. Government retains a nonexclusive, royalty-free license to publish or reproduce the published form of this contribution or to allow others to do so, for U.S. Government purposes.

The Los Alamos National Laboratory requests that the publisher identify this article as work performed under the auspices of the U.S. Department of Energy.

UNCLASSIFIED

*Handwritten initials*

Los Alamos Los Alamos National Laboratory  
Los Alamos, New Mexico 87545

**DESIGN AND OPERATING EXPERIENCE OF AN AC-DC POWER CONVERTER  
FOR A SUPERCONDUCTING MAGNETIC ENERGY STORAGE UNIT**

H. J. BOENIG, Member, IEEE, R. G. NIELSEN, Member, IEEE, AND K. H. SUEKER

**ABSTRACT**—The design philosophy and the operating behavior of a 5.5 kA,  $\pm 2.5$  kV converter, being the electrical interface between a high voltage transmission system and a 30 MJ superconducting coil, are documented in this paper. Converter short circuit tests, load tests under various control conditions, dc breaker tests for magnet current interruption, and converter failure modes are described.

**1. INTRODUCTION**

A 30 MJ superconducting magnetic energy storage (SMES) system was commissioned and field tested in 1983 in Tacoma, Washington, to be used as a tool for system identification and transmission line stabilization [1,2]. The unit consists of three major components: a 2.6 H, 30 MJ superconducting coil mounted in its cryogenic vessel, a closed cycle helium refrigerator that maintains the coil at an operating temperature of 4.5 K, and a twelve-pulse line commutated converter. The converter, which is connected to a 13.8 kV bus via two 6 MVA transformers, regulates the power flow between the coil and the three phase system. Figure 1 shows a circuit diagram of the SMES unit. The two 0A/FA oil cooled transformers have a rating of 6/7.5 MVA, a voltage ratio of 13.8/0.925, and a short circuit impedance of 8.8%. Each transformer is connected to a six-pulse bridge. The two bridges are connected in series and grounded at the center point. The management of the large amount of energy stored in the coil requires a bypass path for each bridge. In the case of a catastrophic failure, the dc breaker can interrupt the coil current by commutating the coil current into a 1  $\Omega$  resistor.

A SMES system can absorb electrical energy and store it in the form of magnetic energy in the coil and release magnetic energy from the coil back into the electrical system. Because the converter allows only unidirectional current flow, the energy flow in the SMES system is controlled by the converter voltage. Positive converter voltage increases the coil current and charges the magnet; negative converter voltage

decreases the coil current and discharges the magnet. After an initial charge to 4.5 kA, the coil current of the 30 MJ coil is controlled between 4 kA and 5 kA. Occasionally, currents up to 5.5 kA must also be accommodated.

Figure 2 depicts the physical installation of the converter flanked by the two power transformers. The thyristors of each converter bridge are mounted on the inner aspect of the converter walls, which are adjacent to the transformers. The dc breaker is housed at one end of the converter cabinet, below the 1  $\Omega$  dump resistor. The dump resistor is mounted on the roof of the converter in a separate drip-proof compartment. The six ac busses and the two dc busses exit the cabinet through the roof.

**2. CONVERTER DESIGN**

**2.1 Circuit, Layout, and Thyristor Selection**

The high power rating of the converter and the objective of running the SMES system at reduced power during a minor converter failure dictate a twelve-pulse circuit. The voltage rating of  $\pm 2.5$  kV makes a series connection of two six-pulse bridges more attractive than a parallel connection, because a 1250 V bridge output voltage can be handled by one high voltage SCR in each bridge leg. The two series connected bridges have the additional advantage that both bridges can be controlled independently. The current requirement necessitates the use of paralleled devices. Each independent bridge is fed by its own transformer. Both transformers have a delta secondary winding, while one primary winding is delta and the other was connected.

In 1978, when the thyristors were purchased, a 50 mm device with a repetitive blocking voltage of 3200 V and an average current of 800 A was selected. This device had, at that time, the highest blocking voltage of any 50 mm SCR wafer produced by an American manufacturer. The thyristor voltage safety factor, defined as the ratio of peak forward or reverse repetitive blocking voltage to rated peak line voltage, equals 2.44 in this application and provides adequate protection for the SCRs with appropriate snubber

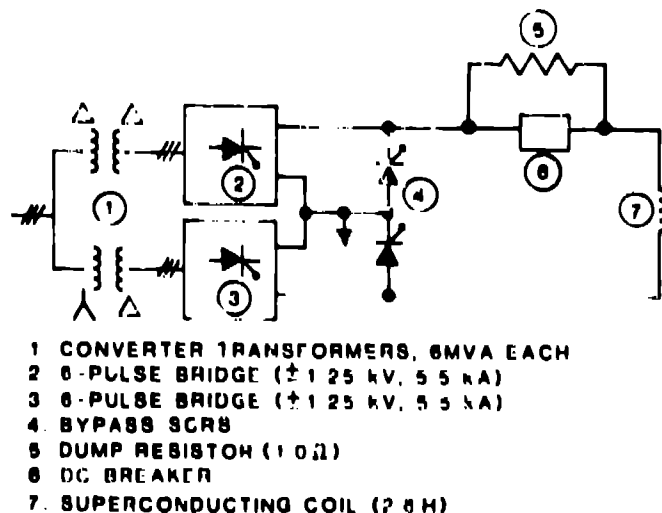


Fig. 1. SMES unit circuit diagram.



Fig. 2. Converter for 30 MJ SMES unit.

networks and metal oxide varistor transient suppression elements installed.

When the number of parallel thyristors in one bridge leg was determined, the one-half-cycle short circuit current through the bridge and not the steady state current was found to determine the minimum number of parallel SCRs. For zero impedance of the 13.8 kV bus and negligible converter impedance, the transformer short circuit current, which occurs when an SCR fails to block, can be calculated to be 42.6 kA. To this value, the maximum dc current must be added to cover the maximum current situation. This short circuit current requires eight SCRs in parallel in each bridge leg. Six SCRs in parallel are required to provide the 5.5 kA steady state current.

The 30 MJ SMES system is installed in a substation which is manned only part of the day. All components must be very reliable, as simple maintenance tasks cannot be performed on a routine basis. The converter housing chosen is suitable for an outside installation. Forced air cooling is preferred over water cooling for better reliability.

## 2.2 Cooling

Semiconductor cooling and air handling are major design considerations. The relatively large number of thyristors makes it economically unattractive to install individual fans to provide high velocity air across the heat sink fins. The decision was made to install the thyristors on the outer sides of the cabinet with the heat sinks angled to permit access. The heat sinks are shrouded to direct air flow, and spaces between sinks are baffled. The entire inside area of the cabinet is pressurized by a centrifugal blower and the heat sinks are allowed to exhaust to atmospheric pressure. Pressure loss through the sinks is high enough so that all other air flow paths present little additional loss. A design minimum air velocity across the sinks of 500 linear feet per minute was confirmed by anemometer measurements. Provisions were made in the mechanical design to permit the installation of balancing dampers, which later proved unnecessary.

Two centrifugal air blowers with a capacity of 20,000 cfm, each driven by a 20 hp motor, are installed to cool the unit. The blowers are sized with sufficient margin to allow some filter pressure loss from dirt accumulation. Only one blower is required at any time, with the second blower in an automatic standby condition.

## 2.3 Current Sharing

Large air-cooled converters present special problems with current sharing among paralleled devices. Balancing transformer arrangements used with water cooled thyristors or diodes become cumbersome and expensive with an air-cooled bus. Sharing can be obtained with large linear inductors in series with ac lines to each thyristor path, but again, economics make this an unattractive option. The path chosen for this design is to match thyristor forward voltage drops within  $\pm 200$  mV and then use small (4.5  $\mu$ H) linear inductors to force a satisfactory balance. These inductors also tend to minimize current imbalances which arise from inevitable differences in commutating inductances of the various bus paths.

It should be noted that equalization of junction temperature rise is the real objective of sharing techniques rather than current balance, per se. For example, a thyristor that has a lower forward voltage drop will tend to have a higher current. However, this device can tolerate a somewhat higher forward current without incurring excessive temperature rise. This property is used to allow smaller inductors than would be required for heat current balance.

The linear inductors allow a relatively fixed current difference which decreases their balancing effectiveness at low load currents. Under these conditions, however, current balance is only a matter of academic interest so long as no thyristor has excessive temperature rise. Current measurements at light load confirmed a steadily decreasing current in each thyristor as load current was decreased.

Inductors are made from grain oriented, gapped, silicon iron "C" cores mounted around the ac bus feeds to the plus and minus thyristor pairs. Gap length was chosen to provide linear operation to about 125% of rated current at full load. Thyristor forward voltage drop becomes increasingly resistive at fault currents, so the saturated inductance still provides sufficient sharing for successful clearing of load faults by gate interruption. Each thyristor is fused with an extremely fast acting 1000 A fuse. Design techniques developed by Balenovich and Karstaedt were used for analysis of fault clearing[3].

## 2.4 Gate Firing

The circuit voltages within each of the series connected six-pulse converter sections allow the use of toroidal pulse transformers for gate drive. These transformers, driven by transistor circuits, are used to provide a continuous drive of 120 electrical degrees in each conduction period. A capacitor discharge circuit provides a fast rise time and overdrive to insure sufficient di/dt capability. The high operating voltages of two converters in series and the possibility of load transients, however, precludes the use of these transformers for the 5 kV class common mode isolation from ground.

High voltage control circuits are supplied from two 120 V isolation transformers, one for each converter section. All gate drive, feedback, and annunciation circuitry associated with each converter section is powered from the isolation transformer. Fiber optic couplers are then used to couple signals to and from ground level control circuits. This system of gate drive was first used on a large tokamak converter system with a 10 kV hipot requirement to ground, and has subsequently been used to provide 15 kV class isolation. No unusual operating problems have been encountered, although some optical links have failed because of LED deterioration with age.

## 2.5 Feedback

Current feedback signals are taken from an instrumentation amplifier connected to a 50 mV shunt. The amplified signal is used to drive an A/D converter which then provides a 10 bit input to a high speed asynchronous parallel/serial converter (PASC). The UART serial output is coupled through an optical link to a low level UART and a P/A converter. Voltage feedback is taken from a resistance divider and encoded in the same fashion as the current feedback. Both links employ dead times between successive words so that the system cannot synchronize incorrectly on a fixed data pattern. The two channels of analog feedback have a bandwidth of 5 kHz.

## 2.6 Bypass Thyristors

The design of any converter system supplying a large magnet must necessarily involve a fail-safe system for managing magnet energy under abnormal conditions. In a converter without a bypass path, loss of ac line would result in load current being trapped in one phase of the converter.

Generally, it is not an economically sound design to size the converter thyristor paths to handle the continuous load current for the long times required to discharge high energy magnets. On the other hand, it is not possible to use a diode bypass path and

regenerate through the bridge by reversing voltage polarity. The method used in this design is to install a thyristor bypass path which can be gated on demand. Resistors (2 m $\Omega$ ) are used to force current sharing in the eight paralleled thyristors.

Two independent gating systems are used in the bypass path. One, driven by a number of fault detectors in the converter (loss of line, low line voltage, phase loss, over temperature, overcurrent, etc.) is coupled through optically isolated gate drivers. Because these drivers obtain their power from the ac source and have no battery backup or uninterruptible power supply, a second completely independent system is used for safety. This system consists of a bus overvoltage detector which triggers a separate gate firing circuit. Power for this circuit is derived from a frequency compensated voltage divider driven by magnet voltage. Again, the technique had previously been proven on converters for large tokamak magnets.

### 2.7 Transient Protection

Both RC filter networks and metal oxide varistors (MOVs) are used for transient protection. The RC filter networks, 2.5 ohms and 15  $\mu$ F per leg, are made from commutating grade, oil filled capacitors and non-inductive resistors. The resistors are made of stainless steel expanded metal, a construction which combines very low inductance with excellent heat dissipation capability. These networks are wye connected to the incoming transformer busses with short cables. MOV devices were the largest low voltage types available at construction time. Two 480 V MOVs are series connected via a delta configuration to suppress incoming transients. The RC networks act to reduce  $dv/dt$  of disturbances, limit thyristor recovery transients and relieve the MOV devices from this duty. In addition, each bridge output voltage is protected by two 575 MOVs connected in series. Voltage surge protection for each thyristor is provided by two series connected 480 V MOVs and an RC snubber network (25  $\Omega$ , 0.1  $\mu$ F) placed across each SCR to bypass voltage spikes and limit  $dv/dt$  across the SCR to prevent misfiring.

### 2.8 DC Breaker Design

In the case of a catastrophic failure, when a line outage or a converter malfunction is followed by a cryogenic system failure, such as loss of vacuum, the coil must be discharged by opening a dc breaker, which transfers the coil current into a resistor. Under normal operation, the dc breaker is closed. A 1  $\Omega$  resistor was found to be large enough to give adequate coil protection. Because a dc breaker for ratings greater than 3 kV and 4 kA was not readily available commercially, a breaker was designed with the known technique of forced current zero and installed in the converter cabinet<sup>[4]</sup>. The parallel connected contacts of an ac power vacuum breaker are used to carry the coil current. When these contacts are opened, a forced current zero is introduced to extinguish the arc between the contacts. A commutation current of 8 kA peak, which causes the main current to go to zero, is generated by discharging a 130  $\mu$ F capacitor through a 15  $\mu$ H inductance into the arcing vacuum contacts. Four series connected 3200 V thyristors withstand, under normal operating conditions, the capacitor voltage of up to 8 kV and are fired to initiate the counter current. A saturable inductor with 0.1 Va rating is installed in series with the three vacuum contacts to reduce the  $di/dt$  value of the breaker current at low current values to ensure the arc will extinguish.  $dv/dt$  using SCRs instead of an ignitron in the commutation circuit, it was hoped to have a more reliable design with less maintenance required. However, the design parameters had to be carefully chosen to stay within the ratings of the SCRs. Based upon the published

one-half cycle, 3-cycle and 10-cycle, 60 Hz surge current ratings, it was felt that a single pulse, sinusoidal commutation current with a peak of 8 kA and a base time length of 300  $\mu$ s could be carried by the device. The  $di/dt$  value for the pulse is 80 A/ $\mu$ s, which is one fifth of the rated minimum value. Equal voltage distribution across the four SCRs connected in series is forced by a resistive network. In addition, each SCR is protected against overvoltages by an MOV device. The firing circuits for the SCRs, including the fiber optic link, were checked for equal pulse delay.

Because of the small size of the capacitor charging supply (30 J/s), which charges the 130  $\mu$ F commutation capacitor in about 20 minutes, a second chance for dc current interruption is not provided. Automatic reclosing eight seconds after breaker opening was arranged in the breaker control logic. The time of eight seconds is the minimum time for the spring loading mechanism of the breaker to reclose. If the dc breaker has functioned properly, only 4.6% of the original current is left in the coil at reclosing time. Should the dc breaker fail, for any given reason, the coil energy would be deposited in the vacuum bottles and result in a breaker explosion. However, by reclosing the breaker, an energy of only 200 kJ, assuming an arc voltage of 40 V, would have been deposited in the three vacuum bottles within eight seconds. This energy is not large enough to destroy the breaker. It is assumed that after breaker malfunctioning, the coil energy is converted into heat in the helium bath and results in excessive helium boil-off without destroying the coil.

## 3. TESTS

### 3.1 Pre-Installation Tests

The converter was tested during acceptance tests at the manufacturer's plant according to the ANSI standards for Semiconductor Power Rectifiers. Two main tests were performed: a short circuit test at 10% overcurrent: 6 kA, for three hours and a no-load test at 10% overvoltage, 1375 V, for five minutes. In addition, the unit was high potted at 19 kV dc. At Los Alamos, the converter was tested at rated current with a voltage up to 150 V and at 240 V with a current of 3.6 kA. A water cooled, stainless steel resistor was used as a load. The high current tests were performed mainly to measure current sharing between the eight parallel thyristors of each bridge leg. These results have been reported earlier<sup>[5]</sup>. Because of limited load capabilities at the manufacturer's plant and at Los Alamos, high power tests were not performed with the converter until the converter was installed at the substation.

### 3.2 Short-Circuit Test

At the Tacoma Substation, the converter was energized for the first time simultaneously with rated current and voltage in a short circuit test. The plus and minus terminals of the converter were connected by a solid aluminum bar, while the superconducting coil remained disconnected. Each six-pulse bridge was first tested separately, with the bypass SCRs of the nonenergized bridge conducting. Figure 3 shows the primary line current  $I_{TL}$  in the wye-delta transformer under short-circuit conditions.

The peak positive current is 560 A, resulting in a peak secondary current of 6977 A. This current value is also the peak SCR current in each bridge leg. The current is determined by the bridge delay angle, which is close to 90°, and the line, transformer, and converter impedances. The line current of the converter with both bridges connected in series and the dc output shorted is shown in Fig. 4. The amplitude of the current harmonics is included for the latter case in

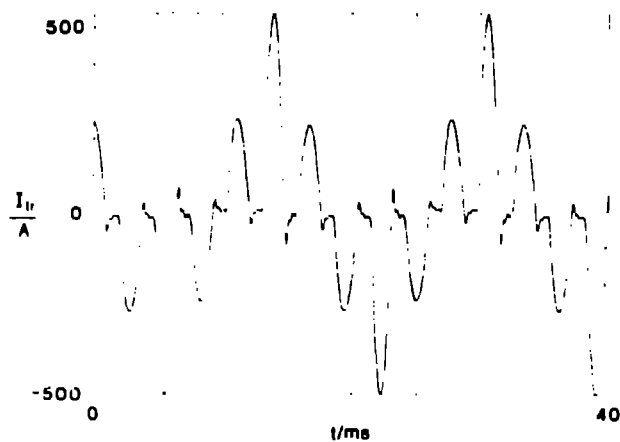


Fig. 3. Transformer primary current with six-pulse bridge short circuited.

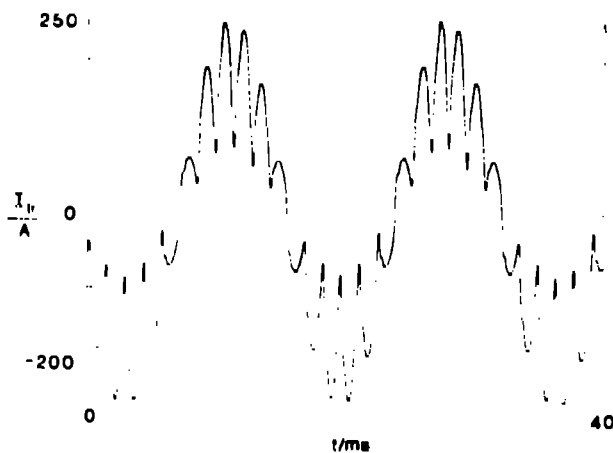


Fig. 4. Transformer primary current with twelve-pulse bridge short circuited.

Table I, showing the dominance of the eleventh and thirteenth harmonics. The slight irregularities of the current pulses are caused by small deviations of the firing angles between the phases of a bridge.

TABLE I

Harmonic Current Measurement

(Transformer Primary Current  $I_{TP} = 155.718A$ )

Harmonic No.	Freq.	Primary Current	Harmonic No.	Freq.	Primary Current
1	60	138.933	15	900	.587
2	120	2.701	16	960	1.105
3	180	4.785	17	1020	.387
4	240	.567	18	1080	.940
5	300	1.077	19	1140	.568
6	360	2.778	20	1200	.906
7	420	1.525	21	1260	.526
8	480	2.346	22	1320	.420
9	540	1.303	23	1380	10.956
10	600	.801	24	1440	.368
11	660	41.752	25	1500	4.490
12	720	.546	26	1560	.238
13	780	18.334	27	1620	.335
14	840	.366	28	1680	.695

### 3.3 Load Tests

#### 3.31 Inversion End Stop

In a SMES system, it is desirable to have the maximum positive and negative converter output voltages as close to equal as possible. While the positive converter output voltage is determined solely by the incoming transformer voltage and the voltage drop due to converter loading, the negative output voltage is determined by the transformer voltage, the voltage increase due to converter loading, and the inversion end stop, which limits the phase delay angle to values considerably lower than  $180^\circ$ . A  $40^\circ$  safety angle proved not too conservative. According to the manufacturer's information, 90% of the SCRs, statistically, have a turn-off time of less than 600  $\mu s$ , which corresponds to an angle of  $13^\circ$ . At  $140^\circ$ , the overlap angle is about  $10^\circ$  as shown in Fig. 5, which depicts the voltage across an SCR. The delay angle  $\alpha$  for this case is  $41^\circ$ , the conduction time is  $129^\circ$  at a dc current of 4.5 kA, and the overlap angle of  $9^\circ$ . The  $18^\circ$  safety margin gives allowance for safe current commutation of dc currents up to 5.5 kA at a reduced voltage level. The 13.8 kV SMES bus is shared with a large aluminum reduction plant having a fluctuating load. It was found experimentally that, while equal delay angle operation of both bridges allowed an inversion end stop of  $145^\circ$ , an end stop of  $140^\circ$  was necessary for independent bridge control.

#### 3.32 Power Tests

The SMES system was used for injecting and absorbing real power pulses into a high voltage transmission system with the aim of identifying power system parameters. Months tests were performed by injecting either sinusoidal, low frequency (0.1 to 1.2 Hz), real power pulses or a narrow band noise power signal into the electrical system. When sinusoidal power pulses are injected, the two independently controlled six-pulse bridges of the converter can assume either an equal or a different phase delay angle. With equal phase delay angles, a real power variation also causes a reactive power variation, while with independent bridge control, the reactive power can be kept constant [2]. Figures 6, 7, and 8 show, in strip chart recordings, three different converter loading conditions. Each recording depicts the bridge 1 voltage ( $V_{d1}$ ), bridge 2 voltage ( $V_{d2}$ ), the converter output current ( $I_d$ ), which is identical to the coil current, and the real ( $P_{SMES}$ ) and reactive ( $Q_{SMES}$ ) power of the SMES unit measured at the 13.8 kV bus. In Fig. 6, the SMES unit follows a sinusoidal power demand signal and both bridges have equal voltage output. The fundamental and second harmonic reactive power variations are significant. In Fig. 7, the SMES unit



Fig. 5. SCR voltage (scale: horizontal 2.02 ms/cm, vertical 725 V/cm).

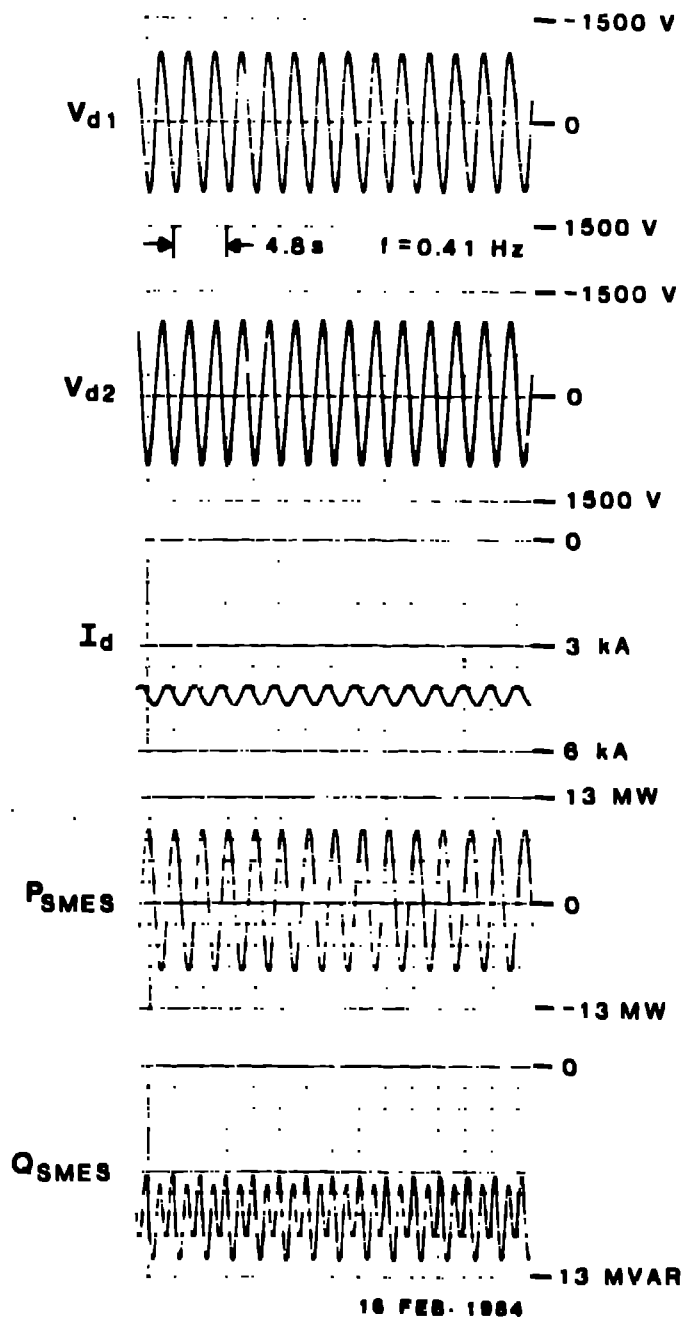


Fig. 6. Electrical parameters of SMES system with sinusoidal power output (equal voltage control).

also puts out sinusoidal real power, but the two bridges are controlled independently and provide a constant reactive power absorption. It should be noted that in Fig. 7, the SMES real power slowly increases and one bridge operates almost exclusively in the rectifier mode, while the other bridge operates in the inverter mode. In Fig. 8, the SMES unit follows a narrow band noise signal demand. The bridges are controlled with equal phase delay angle. The voltage traces show that both positive and negative maximum voltages are reached.

### 3.33 Losses

When the magnet is being charged, the 11.8 kV bus supplies the transformer, converter, and busbar losses and the magnetic energy stored in the coil. When the magnet is being discharged, these losses are supplied by the magnetic energy of the coil. The losses of the

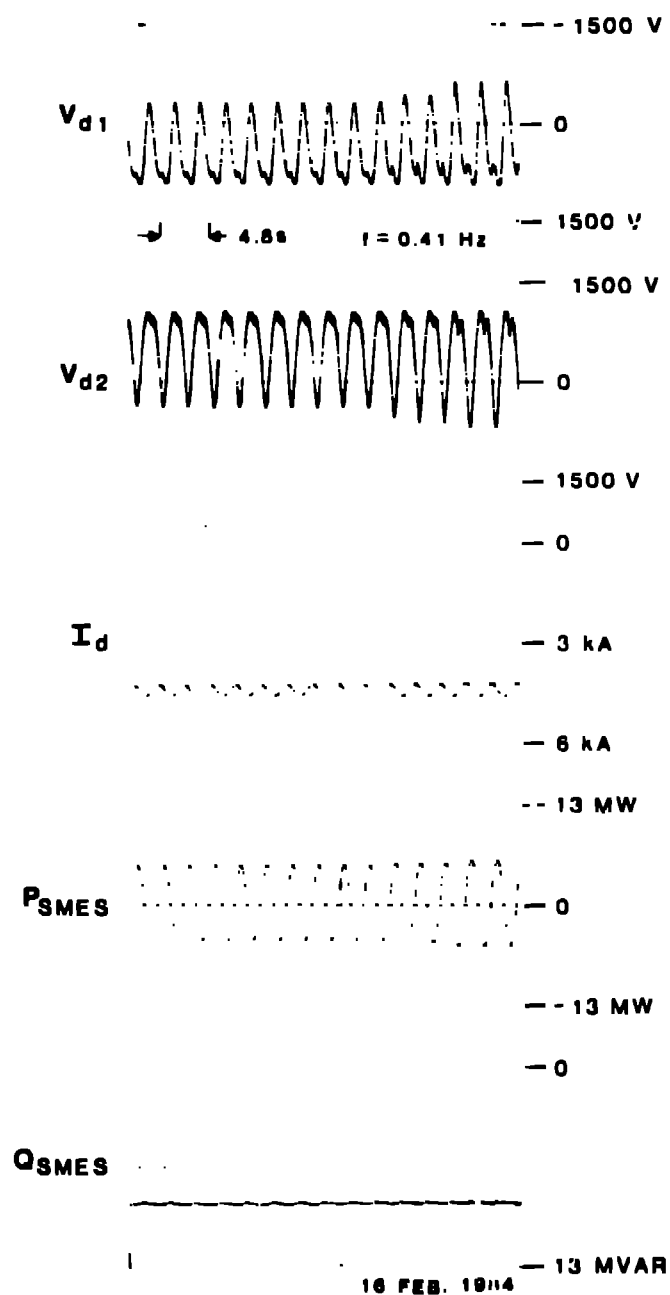


Fig. 7. Electrical parameters of SMES system with sinusoidal power output (constant Q control).

30 MJ SMES unit as a function of constant converter current were measured and are shown in Fig. 9. The losses appear to be linearly dependent on the load current. The graph does not include the 20 hp fan motor or the 1.5 kW control power. The linear relationship between losses and load current can be explained by the fact that the thyristor loss due to the threshold voltage is considerably larger than the loss component due to the thyristor slope resistance. Because the load current varies in time from 4 kA to 5 kA and back to 4 kA during a charge-discharge cycle of the 30 MJ SMES unit, a cycle efficiency of between 97% and 98% can be calculated for the transformers and converter. If the converter of the 30 MJ unit would be connected to a resistive load, the combined converter and transformer efficiency would be 97% at 5 kA load current. This efficiency includes the blower and control power losses.

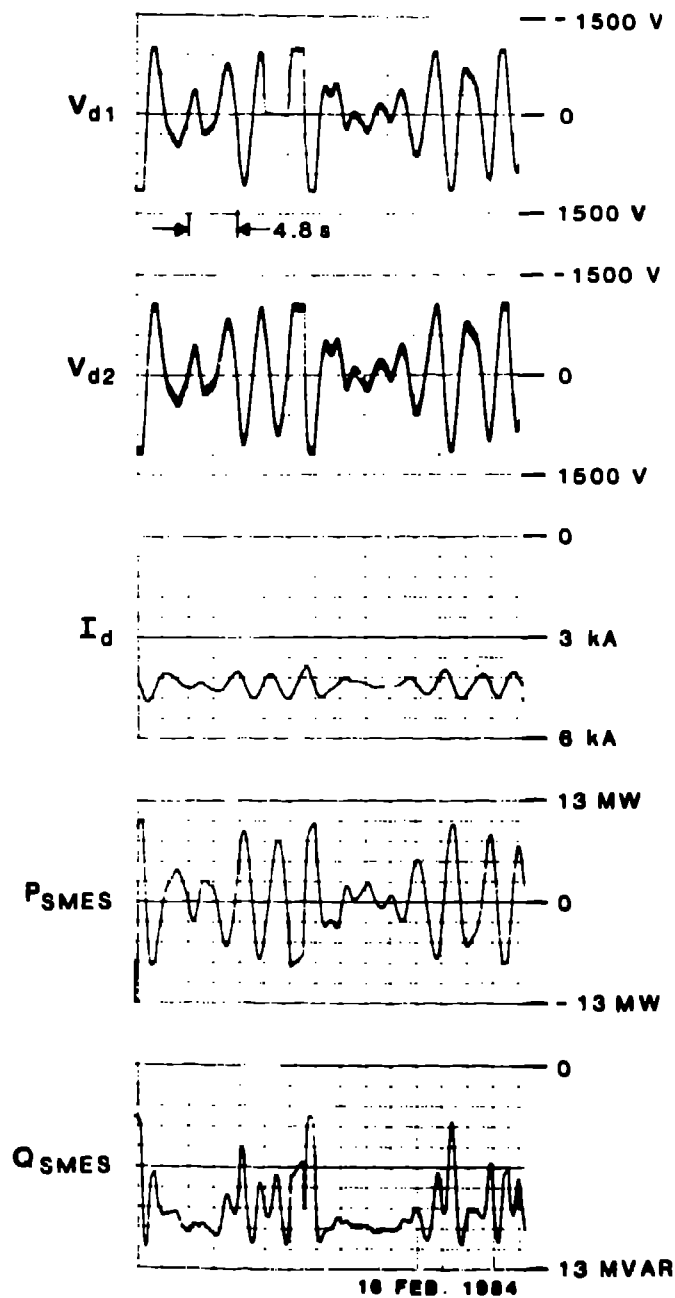


Fig. 8. Electrical parameters of SMES system with random noise signal power output.

#### 3.14 Converter Performance

The converter performed well during continuous duty operation. At full power rating, the converter ran cool with an average temperature difference of  $15^{\circ}\text{C}$  between the incoming and exiting air. Three of the 96 converter SCRs failed during the initial tests. Additional SCRs failed during experiments in which the inversion end stop was increased beyond  $140^{\circ}$ . In one instance, a mechanical malfunction in the 13.8 kV breaker mechanism caused contact bouncing during a breaker closing operation, which resulted in destruction of the RC filter networks and MOV transient suppression devices. However, during this severe voltage transient, none of the converter SCRs was damaged. The electronic logic and relay logic appeared to be quite immune to electromagnetic noise, although

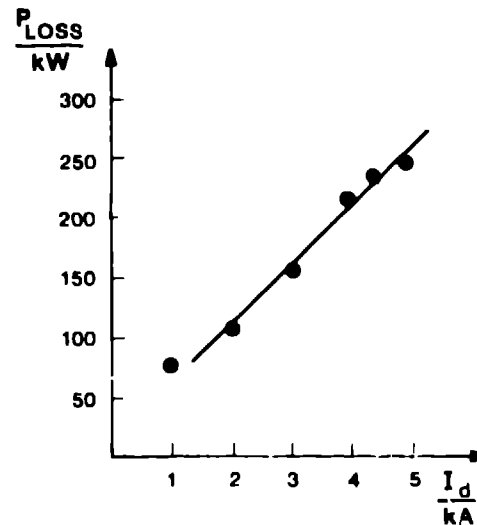


Fig. 9. Converter losses as a function of load current.

some difficulty was expected with the digital circuitry in a noisy converter environment, none was experienced in the field. The converter operation was not interrupted by routine operation of adjacent 230 kV power circuit breakers or disconnect switches within the substation. Misfiring of bypass SCRs occurred when both six-pulse bridges were controlled in a constant reactive power mode with bridge 1 operating primarily in the rectifier mode and bridge 2 in the inverter mode. In Fig. 10, two such misfirings are recorded. The voltage across bridge 1 ( $V_{d1}$ ) is reduced to zero because one of the eight bypass SCRs is conducting. Misfiring occurs when the other bridge is at its inversion end stop. The reactive power ( $Q_{SMES}$ ) is reduced to about half its previous value. A reason for the misfiring has not yet been determined. Experiments showed that misfiring could be avoided by choosing a more conservative inversion end stop.

#### 3.4 DC Breaker Tests

The dc breaker must operate during a double-fault condition, when an electrical system failure is concurrent with a cryogenic system failure. Although such a condition never occurred during the lifetime of the 30 MJ SMES system, the breaker was nevertheless tested up to 5 kA. Tests began at a low current rating (1000 A), and then increased by 1000 A to 4000 A. Several tests at 4.5 kA and test at 5 kA were conducted. Initially, the commutation capacitor charging voltage was adjusted so that the peak commutation current was always approximately 1.6 times the dc current. All breaker tests were successful in that the commutation current extinguished the arc and the magnetic coil energy was deposited in the dump resistor. However, some of the tests at coil currents of 4000 A and above caused a failure in one, two, or all of the commutation SCRs. Initially, an improper design of the SCR MOV protection devices was blamed for the failures. Unfortunately, a visual inspection of the wafers of the damaged SCRs revealed no definite conclusions. Some of the SCRs seemed to have failed because of excessive voltage, others from excessive  $di/dt$ . The cause of the failures was finally determined as time differences in the gate pulses of up to 15  $\mu\text{s}$ , caused by LED deterioration in the optical sensor.

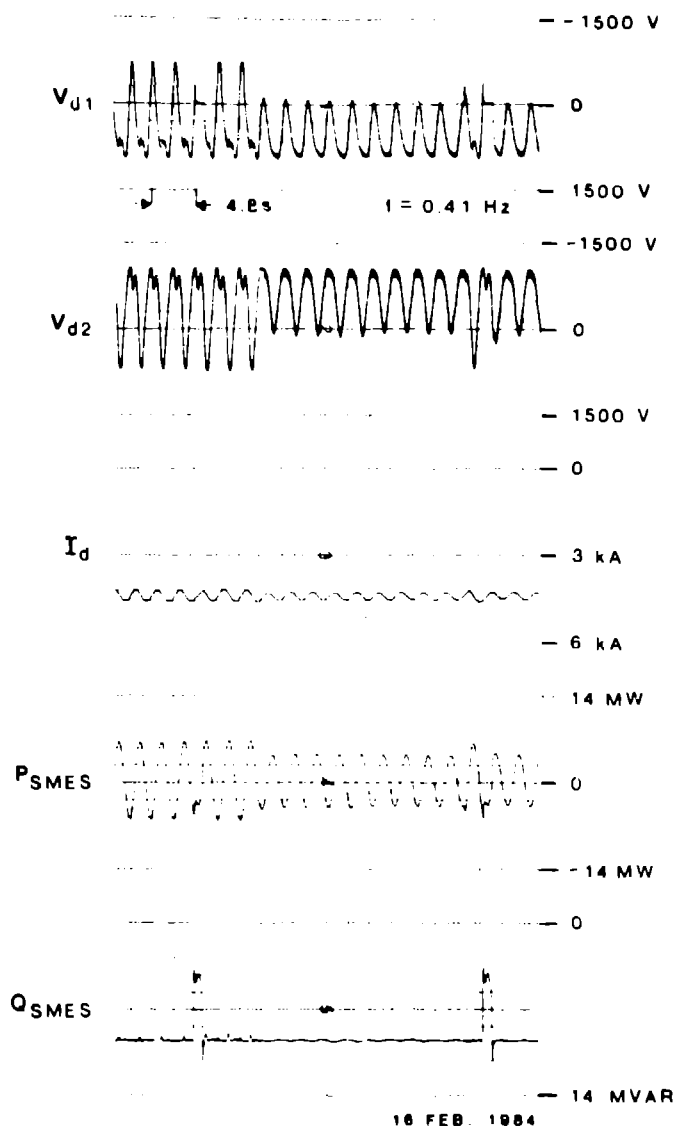


Fig. 10. Electrical parameters of SMES system with misfiring of bypass SCR.

#### ACKNOWLEDGEMENTS

Appreciation is due Dr. J. F. Hauer of the Bonneville Power Administration for his cooperative effort during the testing phase of the 30 MJ SMES unit and Dr. D. P. Hartmann of the Bonneville Power Administration for providing Figs. 3 and 4 and Table 1 for this publication.

#### REFERENCES

1. J. D. Rogers, R. I. Schermer, B. J. Miller, J. F. Hauer, "30 MJ Superconducting Magnetic Energy Storage System for Electric Utility Transmission Stabilization," Proc. of the IEEE, Vol. 71, September 1983, pp. 1099-1107.

2. H. J. Boenig, J. F. Hauer, "Commissioning Tests of the Bonneville Power Administration 30 MJ Superconducting Magnetic Energy Storage Unit," paper presented at IEEE PES, 1984 Summer Power Meeting, Seattle, WA, July 1984.
3. J. D. Balenovich, W. H. Karstaedt, "An SCR Surge Suppression Rating Technique," IEEE IAS 1976 Conf. Record, IEEE Pub. No. CH1122-1-1A, pp. 191-206.
4. T. H. Lee, "Physics and Engineering of High Power Switching Devices," MIT Press, 1975, pp. 397-408.
5. H. J. Boenig, R. D. Turner, C. L. Neft, K. H. Sueker, "Design and Testing of a 13.75 MW Converter for a Superconducting Magnetic Energy Storage System," Proc. 9th Symp. Eng. Prob. of Fusion Res. (Chicago, IL, October 26-29, 1961), IEEE Pub. No. 81CH1715-2 NFS, pp. 452-455.